OPEN ACCESS

University of BRISTOL

Al Mallak, K. A., Nair, M., Hilton, G. (Ed.), Loh, T. H., & Beach, M. A. (2021). Characterising Vehicle Suspension Variations in Millimetre Wave V2I System. In *2021 IEEE 93rd Vehicular Technology Conference, VTC 2021-Spring - Proceedings* [9448901] (IEEE Vehicular Technology Conference; Vol. 2021-April). Institute of Electrical and Electronics Engineers (IEEE). https://doi.org/10.1109/VTC2021-Spring51267.2021.9448901

Peer reviewed version

License (if available):
Unspecified

Link to published version (if available):
10.1109/VTC2021-Spring51267.2021.9448901

Link to publication record in Explore Bristol Research
PDF-document

This is the accepted author manuscript (AAM). The final published version (version of record) is available online via IEEE at 10.1109/VTC2021-Spring51267.2021.9448901. Please refer to any applicable terms of use of the publisher.

University of Bristol - Explore Bristol Research

General rights

This document is made available in accordance with publisher policies. Please cite only the published version using the reference above. Full terms of use are available: http://www.bristol.ac.uk/red/research-policy/pure/user-guides/ebr-terms/

Characterising Vehicle Suspension Variations in Millimetre Wave V2I System

Khalid A Al Mallak[1], Manish Nair[1], Geoffery Hilton[1], Tian Hong Loh[2], Mark Beach[1]
[1] Communications Systems and Network, EPSRC CDT in Communications, University of Bristol (UoB)
Bristol, United Kingdom, {k.almallak, qx20364, geoff.hilton, m.a.beach}@bristol.ac.uk
[2] Electromagnetic & Electrochemical Technologies Department, National Physical Laboratory/NPL,
Teddington, United Kingdom, tian.loh@npl.ac.uk

Abstract—**This paper investigates the effects of antenna vibration occurring due to suspension variation during the movement for vehicle-to-infrastructure (V2I) communication by developing a two dimensional (2D) model. With highly directional antennas fitted on a car's rear bumper and at a base station (BS), different beamwidths from 10° to 50° are investigated for a moving vehicle at 70mph. The gain sensitivity of the radiation pattern and the micro-Doppler shift are modelled for suspension variations between 5cm and 20cm. The analysis has been performed based on the observed angle of arrivals (AoA) at the receiver antenna in the elevation plane. The gain sensitivity represents the BSs' main lobes' misalignments and receiver antennas' radiation patterns at 26GHz. The results reveal a significant impact on gain sensitivity during the first 200m of movement away from the BS. Furthermore, the total Doppler shift increases due to the micro-Doppler with vertical displacements from the suspension variation. However, this can be mitigated if the beamwidth increases relative to the link budget or the BS height increases. The 2D model is validated by utilising accelerometer data recorded whilst the vehicle is moving at 70mph on a motorway, by extracting the displacements and computing the gain sensitivity.**

Index Terms— Antenna's vibration, beamwidth, gain sensitivity, micro-Doppler shift and suspension variation.

I. Introduction

One of the main challenges in vehicle-to-infrastructure (V2I) communications is maintaining the direct link between the base station (BS) and a vehicle. According to [1, 2], a reliable millimetre wave (mmWave) communication link is preserved if there are directional antennas deployed at the BS and the vehicle. It is essential to correctly align directional antennas towards the BS as any antenna's misalignment degrade the communication link [3].

During motion, a vehicle is subject to vibrations produced from the engine and the suspension variations on an uneven road [4]. Vibrations produced from suspension variations cause a displacement relative to time which can be realised by the antennas mounted on the bumper. It changes the gain sensitivity represented by the misalignment of the main lobes of the BS and receiver antennas' radiation pattern over the travelled distance, increases the total Doppler shift and degrades the signal's quality. The novelty of this paper is to investigate how to mitigate the impact of vertical vibrations and the antenna depointing by relating antenna beamwidth to travelled distance on a motorway. This paper is divided into five sections: the background in Section II, a description of a two-dimensional (2D) V2I communications model and Gain sensitivity Algorithm in Section III, results and analysis in Section IV, whilst Section V concludes with the outcomes of this paper and presents some recommendations for future investigation.

II. Background

A. Short and Long-Range Antenna's Vibrations

The short and long-range antenna's vibrations are related to the rate of antenna's displacement occurring relative to time. Short-range vibration reflects driving on potholes which causes sudden antenna displacements. In contrast, a long-range one reflects an environment where a vehicle moves on bumpy roads for a long distance. According to [5], signal power distortion can be mitigated using a high gain horn antenna. Although [5] discussed only short-range vibration at 5.8GHz, the idea is still applicable for higher frequencies like 26GHz. The characterisation of spatial filtering for horn antennas eliminate non-dominant multipath components (MPCs), and the receiver's antenna receives only strong MPCs.

Furthermore, the radiation pattern has power propagating in both azimuth and elevation planes. Therefore, the direction of mechanical vibration influences the direction of the displacement that impacts the radiation pattern. The suspension variations in a vehicle are equivalent to pitching in mechanical motion. However, only the vertical motion is dominant, unlike other mechanical motions such as yawing or rolling. Here, the antenna's vertical polarisation is vital because it detects the suspension variation in the elevation plane. Horizontal polarisation can be considered for studying the vibrations in the azimuth plane and is left for future work. This is similar to yawing in mechanical motion, which is a short-range vibration, rarely occurring due to (i) sudden push from the side because of strong winds, (ii) sudden driving manoeuvres or, (iii) from a destructive road camber.

B. Influence of Antenna's Beamwidth

One of the horn antennas' characteristics is the high gain beamwidth utilised to maintain a highly directional communication between the BS and mobile user equipment (UE). Since V2I communication at mmWave frequencies promises high data-rate and low latency, the bandwidth expected is in multiple GigaHertz, making the receiver susceptible to power variations. Consequently, any change in the gain sensitivity because of the antenna's vibrations will impact the received signal-to-noise ratio (SNR). Therefore, if the beamwidth is appropriately selected, it improves the channel performance by increasing the SNR, enhancing the Rician channel gain, and reducing the RMS-DS [6, 7]. Furthermore, adaptive beamforming in [5], can be implemented to adjust the beamwidth by following the targeted signal's AoA [7]. However, moving the vehicle further away from the BS does not enhance the channel gain in adaptive beamforming because the radiated power itself would be weaker. [7] also considers fixed beamforming that generates narrower fixed beamwidths having higher beam gains to overcome this limitation. This also reduces measurement uncertainties and avoids expensive hardware. Our research's novelty is based on investigating BS heights and applying different beamwidths in a 2D V2I model. A carefully designed BS height guarantees the right coverage area for the mobile UE. Therefore, any change in the gain sensitivity due to vibrations caused by suspension variations will be detected by the receiver's antenna at narrower beamwidths but only for a short distance from the BS. If a wider beamwidth is employed, the horn antenna's gain sensitivity changes cannot be realised.

C. *Impact of Vertical Vibration on the Doppler Shift*

To the best of the authors' knowledge, few studies are available where vibration and the resultant micro-Doppler shift are investigated at 26GHz. The micro-Doppler shift created degrades the baseband signal at the receiver. This is because any vibration occurring during the movement adds additional modulation to the received signal, making it difficult to reconstruct the original signal. The RF bandwidth is also relevant for micro-Doppler estimation because it produces beam squint, which changes the beamwidth and beam direction according to frequency. Vertical displacement occurs because the suspension variation will create an additional Doppler shift referred to as micro-Doppler. Consequently, the total Doppler shift will be higher than the one without vibration. The formulation for the total Doppler shift is derived as [8]

$$f_d = f_c \prod_{i=1}^{n+1} \left(\frac{c - \vec{v_i} \cdot \hat{k}_i}{c - \vec{v}_{i-1} \cdot \hat{k}_i} \right) = f_c \prod_{i=1}^{n+1} f_{d_i} \quad (1)$$

where f_c is the carrier frequency (26GHz), n is the number of the vertical displacement points, v_i is the vertical displacement velocity of a ray after hitting a moving object, and k_i is a unit direction vector that corresponds to a i-th ray associated with the i-th vertical displacement point. Intuitively, the i-th vertical displacement point produces a micro-Doppler shift Δf_{d_i}. The micro-Doppler shift investigated in this research models the difference in Doppler shift with and without vibrations given by

$$\Delta f_d = f_d - f_{d,vertical\ vibration} \quad (2)$$

III. Two Dimensional (2D) Model, Gain Sensitivity Algorithm and Assumptions

The proposed 2D model and the gain sensitivity algorithm generate a radiation pattern for vertical polarisation because the vibration from the vertical suspension is considered here, unlike horizontal vibration during the movement. Different BS Half Power Beam Widths (HPBWs) from 10° to 50° impacted by antenna's aperture are examined, assuming that both the transmit and receive antennas are horn antennas. The heights of the transmit and receiver antennas are h_{tx} and h_{rx}, respectively, which are shown in conjunction with the vertical displacement due to suspension variations dh in Fig. 1. Table I includes realistic and operational scenarios based on LoS communication only and without a blocking vehicle. Further, three h_{tx} heights namely, 10m, 15m and 20m, are

TABLE I

PARAMETERS FOR V2I MODEL WITH SUSPENSION VARIATION

Parameters	Values
BS heights (m)	10, 15, 20
Range/ travelled distance (m)	1 – 500
Sampling time (ms)	31.52
Rx antenna's height from the road (cm), equivalent to a typical height of a car's bumper	45
Suspension variations (cm)	5, 10, 15, 20
BS Beamwidths (degree)	10 - 50
mmWave freq. (GHz)	26
Speed equivalent to 70 mph (m/s)	31.29

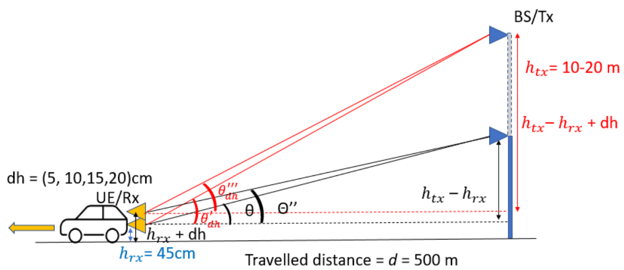

Fig. 1: 2D V2I model for two different BS h_{tx} which are expected to be used by a network infrastructure. The h_{rx} is 45cm which is equivalent to fitting an antenna on a car's bumper in order to detect the suspension variation unlike fitting it on the side mirror or the roof of a vehicle.

investigated. These heights are expected to be deployed with the BS. Moreover, it is assumed that h_{rx} is equal to 45cm, which is equivalent to the height of a personal car's bumper. Other assumptions made to validate the model are choosing suspension variations of 5cm to 20cm while a vehicle moves away from the BS at 70mph and for a distance of 500m. The iterative steps in the 2D modelling are as follows:

The AoAs (θ, θ', θ'', θ''') shown in Fig. 1 are computed without and with vertical displacement dh, and for every single meter, the vehicle moves. These are obtained by simple geometry as

$$\theta = \tan^{-1}(h_{tx} - h_{rx})/d \qquad (3)$$

and

$$\theta_{dh} = \tan^{-1}(h_{tx} - h_{rx} + dh)/d \qquad (4)$$

for $\theta \in \theta, \theta', \theta'', \theta'''$ and $\theta_{dh} \in \theta_{dh}, \theta'_{dh}, \theta''_{dh}, \theta'''_{dh}$. A look-up table is then generated containing beam-gains values $G[b_d(\Theta)]$; for every beam $b_d(\Theta) \in 10^{\circ}{:}50^{\circ}$ as a function of the radiation pattern in elevation plane $\Theta \in 0^{\circ}{:}180^{\circ}$; at every travelled distance d∈1m:500m (see Fig. 1).

From the lookup table, beam-gains $G[b_d(\theta)]$ and $G[b_d(\theta_{dh})]$ at AoAs with and without vertical displacement are selected. The set of gain sensitivities $\mathcal{S}$ in dB are obtained by comparing the looked up gains $G[b_d(\theta)]$ and $G[b_d(\theta_{dh})]$ with and without suspension variations as

$$\mathcal{S} = 20\log_{10}|G[b_d(\theta)] - G[b_d(\theta_{dh})]| \qquad (5)$$

∀θ∈θ, θ^', ", θ''', ∀θ_dh∈θ_dh, θ_dh^', θ_dh^''', θ_dh^''';
∀b_d (θ),b_d (θ_dh)∈10^∘:50^∘ and; ∀d∈1m:500m.

This procedure is summarised in Algorithm 1: Gain Sensitivity Algorithm. Another assumption made is that the extent of vertical vibration is short-range.

Algorithm 1: Gain Sensitivity Algorithm

1: Initialisation: Compute the AoAs without and with vertical displacement dh, θ and θ_{dh} from (3) and (4).
2: for d =1m:500m
3:   **for** $\Theta = 0^{\circ}: 180^{\circ}$
4:   **for** $b = 10^{\circ}{:}50^{\circ}$
5:   obtain look-up table $b_d(\Theta)$, $G[b_d(\Theta)]$
6:   **if** $\theta, \theta_{dh} == \Theta$ **then**
7: $b_d(\Theta) = b_d(\theta)$ **or** $b_d(\Theta) = b_d(\theta_{dh})$
8:   **end if**
9:   **end for**
10:   **end for**
11: end for
12: Obtain the set of directivities $\mathcal{S}$ from (5)

Furthermore, for modelling a realistic short-range scenario, suspension variations of 5cm to 20cm are analysed for up to a travelled distance of 500m in this paper. They reflect the real behaviour of suspension variations occurring due to a vehicle's movement on potholes, as explained previously in Section IIA.

A. Gain Sensitivity

The set of gain sensitivities derived from the Gain Sensitivity Algorithm is applied to produce a 3D matrix showed in Fig. 2, assuming the BS heights are either 10m or 15m. This highest gain sensitivity was when the beamwidth was 10° because this beamwidth causes the most significant antenna depointing impact on the received waveform. This issue is significant, and it is hard for a receiver's antenna boresight to point towards the BS during the first 100m of travelled distance. However, the gain sensitivity drops when the vehicle moves further away from the BS because of a reduced gain observed at the receiver's antenna. Furthermore, in the far-field, the AoAs with and without vertical displacements match each other (step 6-8 in

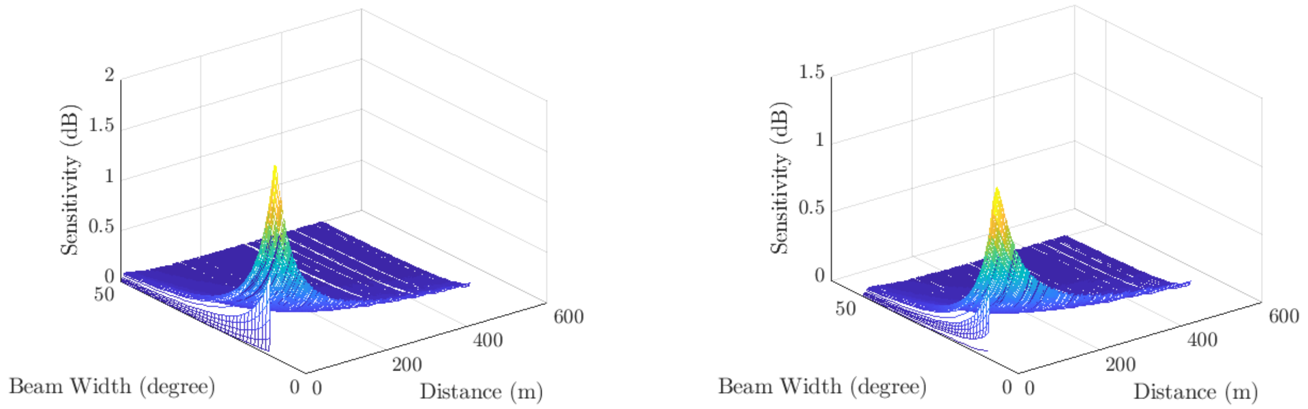

(a) (b)

Fig. 2. 3D graphs where (a) & (b) show the gain sensitivity observed when h_{tx} was 10m and 15m correspondingly. The dh considered was 5cm.

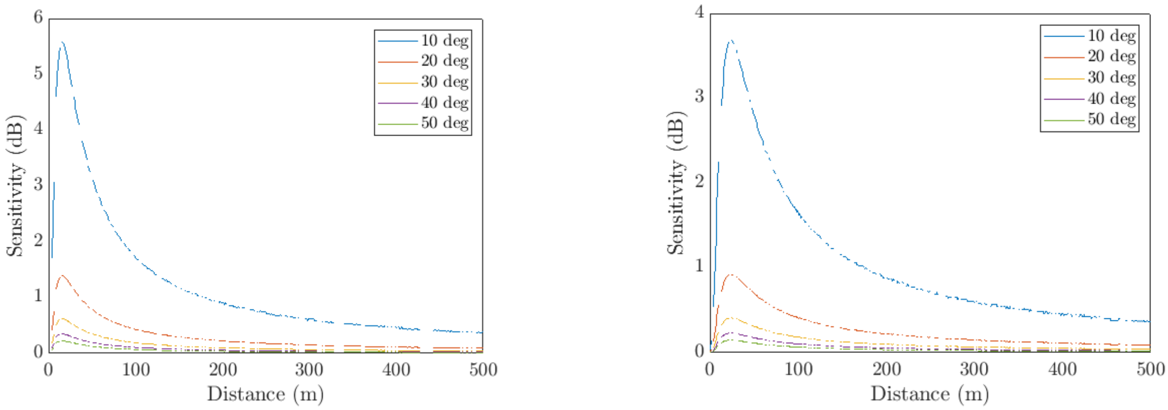

(a) (b)

Fig. 3. Gain Sensitivity vs distance for different BS heights (a) 10m and (b) 15m respectively. In both cases the dh=15cm.

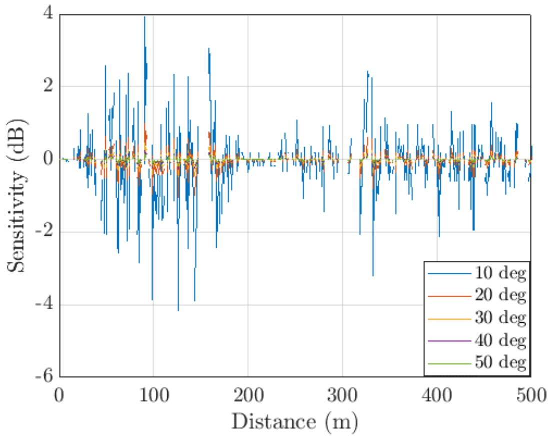

Fig. 4. Gain sensitivity when a vehicle is moving at 70mph on a motorway assuming h_{tx} of 10m from the model and different beamwidths.

Algorithm 1 where the gain corresponding to the AoAs are extracted through the look-up table), resulting in close to zero gain sensitivity. However, after travelling a longer distance, the vertical displacement produced from suspension variations does not influence the received power because the gain sensitivity is near zero. Moreover, the gain sensitivity observed decreases if the BS height $h_{tx} = 15m$. Higher BS enables better coverage of the radiation pattern in the far-field. Therefore, gain sensitivity tends to zero at a travelled distance beyond 200 metres because the differences between elevation angles of the radiation pattern and the AoAs are nearly zero. However, the gain sensitivity is further improved with wider investigated beamwidths from 10° to 50°. This will provide border coverage of radiation power at farthest travelled distances. However, it necessitates a trade-off between increasing the beamwidth and maintaining the mmWave antenna's high directivity to ensure that the impact of suspension variation is mitigated. Furthermore, to investigate how BS height impacts the gain sensitivity, for h_{tx} of 10m, the gain sensitivity is nearly 5.6dB, whilst for h_{tx} of 15m, the gain sensitivity is nearly 3.6dB. Fig. 3a and Fig. 3b present the gain sensitivity against the travelled distance for different beamwidths, at h_{tx} of 10m and 15m correspondingly.

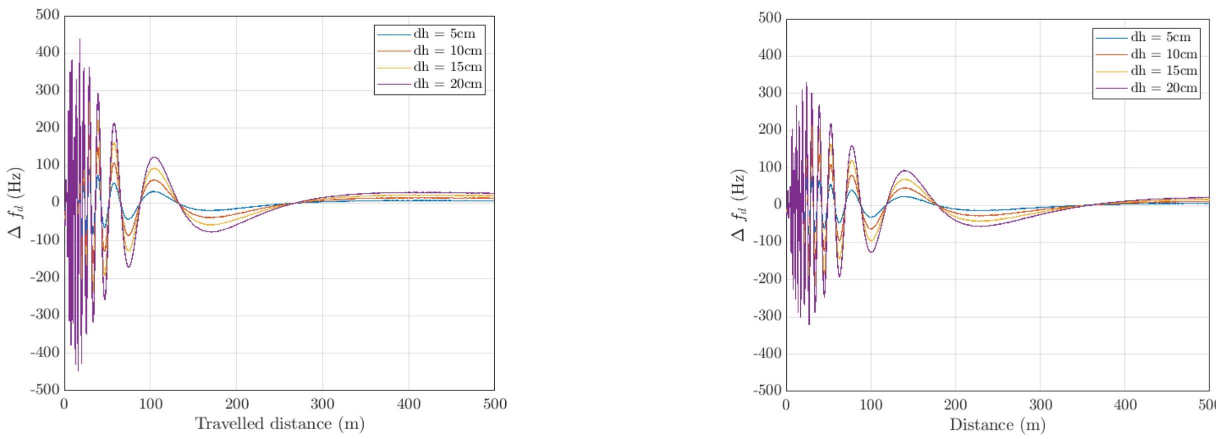

(a) (b)

Fig. 5: Δf_d for BS heights of (a) 15m and (b) 20m respectively. The frequency of fluctuation decreases with the distance because the gain of radiation pattern decreases and becomes close to zero. Therefore, the effect of the suspension variation becomes non-significant by travelling further away from the BS.

It indicates that the BS height has a significant role in improving the power sensitivity. Moreover, a lower BS height results in high gain sensitivity because of suspension variations during movement. However, this observation holds only during the first 100m travelled and drops beyond this distance. Beyond 100m, the gain sensitivity drops to near zero, as explained previously. Further, the narrower beamwidth of 10° would show high gain sensitivity compared to other investigated beamwidths explaining a mmWave horn antenna's spatial filtering characteristic, eliminating any MPCs outside the antenna facets. The model is validated by applying displacement data extracted from an accelerometer in order to compute the AoAs. This acceleration is recorded by using an iPhone application. The iPhone is mounted on the dashboard of the vehicle moving at 70mph on the motorway. The acceleration is recorded for 3.26 minutes which corresponds to travelling a distance of 6536m. However, the gain sensitivity estimated from the 2D model covers the first 500m, which lasts for 15.76s as depicted in Fig. 4, assuming the BS heights h_{tx} of 10m and HPBWs $10°, 20°, 30°, 40°$ and $50°$. The oscillation is pertinent to the suspension variation occurring during the movement. The 15cm suspension variation could be seen if the road is a bumpy one and will augment by travelling a longer distance at a constant speed. However, the accelerometer showed instantaneous oscillation related to suspension variation during the movement, as reflected in the gain sensitivity estimated from the 2D model in Fig. 4.

B. Doppler Shift

It is imperative to investigate the change in Doppler shift when there is a vertical vibration of the antenna, as the Doppler shift has a direct impact on the mmWave signal primarily when a vehicular channel has investigated. This is because of the additional modulation added to the received signal. Based on the 2D model in Fig.1 and the vehicle's modelled velocity of 70mph, the maximum Doppler shift is computed at 26GHz. A negative Doppler shift is studied because the car is moving away from the BS. To calculate micro-Doppler shift, the AoAs $\theta \in \theta, \theta', \theta'', \theta'''$ and $\theta_{dh} \in \theta_{dh}, \theta_{dh}', \theta_{dh}'', \theta_{dh}''''$ in the 2D model, $\theta_{dh}, \theta_{dh}', \theta_{dh}'', \theta_{dh}''''$ in the 2D model are utilised to calculate the f_d and $f_{d(vertical\, vibration)}$ for each dh, h_{tx} and h_{rx} by using equation (1). The set of Doppler shifts are

$$f_d = -\frac{v.f}{c}\cos(\theta) \quad (6)$$

$$f_{d,vertical\, vibration} = -\frac{v.f}{c}\cos(\theta_{dh}) \quad (7)$$

where v is the velocity of the vehicle.

However, the micro-Doppler shift produced from the vibration can be minimised using low pass filters (LPFs) [9].

IV. CONCLUSIONS AND RECOMMENDATIONS

Antenna's displacement occurring from vibration or suspension variation impacts the gain sensitivity represented by the radiation pattern. This issue is mitigated using beamwidths higher than 10° or by increasing the BS height by a few meters based on the 2D model and Gain sensitivity Algorithm. Further, the Doppler shift increases when vibration occurs, impacting the received signal quality as it causes the antenna's depointing. This issue will be significant for V2I communication analysis as vibration is inevitable. This research can be further expanded to include investigating the impact of horizontal vibration in the azimuth plane and would be used in future publications. It shows that the type of vehicle suspension system and the antenna's position in a modern vehicle will play a vital role in stabilising the vehicle's body. Nevertheless, fitting the antenna on the roof of a vehicle or the side mirrors will be considered a rigid body that does not detect the suspension system and require further investigation.

REFERENCES

[1] J. Blumenstein *et al.*, "In-Vehicle Channel Measurement, Characterization, and Spatial Consistency Comparison of 3-11 GHz and 55-65 GHz Frequency Bands," *Vehicular Technology, IEEE Transactions on,* vol. 66, no. 5, pp. 3526-3537, 2017, doi: 10.1109/TVT.2016.2600101.

[2] B. Antonescu, M. T. Moayyed, and S. Basagni, "mmWave channel propagation modeling for V2X communication systems," vol. 2017-, ed, 2017, pp. 1-6.

[3] L. Simić, N. Perpinias, and M. Petrova, "60 GHz Outdoor Urban Measurement Study of the Feasibility of Multi-Gbps mm-Wave Cellular Networks," 2016.

[4] J. Blumenstein, J. Vychodil, M. Pospisil, T. Mikulasek, and A. Prokes, "Effects of vehicle vibrations on mm-wave channel: Doppler spread and correlative channel sounding," in *2016 IEEE 27th Annual International Symposium on Personal, Indoor, and Mobile Radio Communications (PIMRC)*, 4-8 Sept. 2016 2016, pp. 1-5, doi: 10.1109/PIMRC.2016.7794619.

[5] C. Nieh, T. Huang, and J. Lin, "Antenna radiation pattern effects on a short-range vibration-detection radar system," in *2014 International Symposium on Antennas and Propagation Conference Proceedings*, 2-5 Dec. 2014 2014, pp. 135-136, doi: 10.1109/ISANP.2014.7026567.

[6] V. Va, T. Shimizu, G. Bansal, and R. W. Heath, "Beam design for beam switching based millimeter wave vehicle-to-infrastructure communications," in *2016 IEEE International Conference on Communications (ICC)*, 22-27 May 2016 2016, pp. 1-6, doi: 10.1109/ICC.2016.7511414.

[7] G. Yue *et al.*, "Millimeter-Wave System for High-Speed Train Communications Between Train and Trackside: System Design and Channel Measurements," *IEEE Transactions on Vehicular Technology,* vol. 68, no. 12, pp. 11746-11761, 2019, doi: 10.1109/TVT.2019.2919625.

[8] D. Bilibashi, E. M. Vitucci, and V. Degli-Esposti, "Dynamic Ray Tracing: Introduction and Concept," in *2020 14th European Conference on Antennas and Propagation (EuCAP)*, 15-20 March 2020 2020, pp. 1-5, doi: 10.23919/EuCAP48036.2020.9135577.

[9] V. C. Chen, F. Li, S. Ho, and H. Wechsler, "Micro-Doppler effect in radar: phenomenon, model, and simulation study," *IEEE Transactions on Aerospace and Electronic Systems,* vol. 42, no. 1, pp. 2-21, 2006, doi: 10.1109/TAES.2006.1603402.